Surface characterization and methylene blue adsorption studies on a mesoporous adsorbent from chemically modified *Areca triandra* palm shell

Hariharan Thangappan[a], Arjun Valiya Parambathu[b], Shiny Joseph[a,*]

[a]*Department of Chemical Engineering, National Institute of Technology Calicut, Kozhikode, India, Tel. +91 9037248499;*
email: vijayhariharan99@gmail.com (H. Thangappan), Tel. +91 495 2285400; Fax: +91 495 2287250;
email: shiny@nitc.ac.in (S. Joseph)
[b]*Department of Chemical Engineering, National Institute of Technology Surathkal, Surathkal, India, Tel. +91 8593853454;*
email: vparjun@yahoo.com

ABSTRACT

Activated carbon was prepared from *Areca triandra* palm shell (ATPS) by chemical activation with sulphuric acid, and its application for the adsorption of methylene blue dye from aqueous solution was investigated. FTIR spectral analysis and Boehm titrations were used to examine the oxygenated surface functional groups tailored to adsorb cationic toxins from solutions, point of zero charge estimated the surface charge for electronic affinity induced by chemical treatment. BET and SEM analyses revealed mesoporous adsorbent with homogenous pores and the BET surface area is 27.3 m^2/g. The influence of process parameters, namely contact time, initial concentration, adsorbent dosage and pH was evaluated by batch adsorption studies. The equilibrium adsorption data were fitted with three isotherm models, among them Langmuir isotherm model best fitted and the maximum adsorption capacity of methylene blue was found to be 312.5 mg/g. The kinetic adsorption data best fitted with pseudo-second-order kinetics out of three kinetic models tested. The thermodynamic parameters, Gibb's free energy change ($\Delta G°$), enthalpy change ($\Delta H°$) and entropy change ($\Delta S°$) ascertain that the adsorption is a spontaneous endothermic process with high affinity between surface and dye. The results of the present study suggest that the adsorbent prepared from ATPS is a potential adsorbent for the treatment of effluent containing cationic dyes.

Keywords: *Areca triandra*; Acid treatment; Activated carbon; Methylene blue; Adsorption

1. Introduction

The demand for good quality drinking water is increasing exponentially due to pollution of streams and underground sources caused by industrialization, urbanization and population growth. The effluents from textile, dye manufacturing, printing and pulp and paper industries are highly coloured and harmful in nature. The discharge of these effluents into the rivers and lakes poses a major threat to aquatic life and reduces light penetration and alters the biological stability of the surrounding ecosystem. Hence, it is very important to treat the coloured dye effluent as they are hazardous to the environment, aquatic life and human being.

*Corresponding author.

It was reported that there are 10,000 different dyes which are synthesized with over 7×10^5 MT of annual production for commercial applications, approximately 15% of these dye stuffs is discharged as effluent while processing [1,2]. Methylene blue dye finds wide usage in dyeing applications of cotton, wool, paper and temporary hair colourant. Methylene blue dye on inhalation causes harmful rapid breathing effect, oral ingestion causes nausea, vomiting, diarrhoea and gastric discomforts. Large doses of intake may result in abdominal pain, chest pain, severe headache, profuse sweating, mental confusion, micturition and methaemoglobinaemia [3–5]. Proper removal of such dyes from the effluent before discharging is a primal obligation of the process industry.

A number of technologies have emerged recently for the removal of pollutants from wastewater, such as photocatalytic degradation, ozonation, electrochemical degradation, flocculation, electrocoagulation, precipitation, ion exchange, membrane filtration and reverse osmosis [6–8]. When it comes to the expense of the equipment and operations, these technologies prove to be disadvantageous for any small-scale industries to implement. The conventional adsorption process is still a cost-effective and well-disposed technique for the removal of traces of such pollutants successfully [9,10].

Adsorption using an activated carbon adsorbent is regarded as the most effective process in the removal of pollutants from aqueous solutions. As it is expensive to employ activated carbon in large-scale purification of dye contaminated wastewater, various low-cost adsorbents such as agricultural waste products in crude and chemically modified form were investigated in order to substitute for activated carbon [11,12].

Different agricultural byproducts such as sago waste, sunflower head, sunflower stem, saw dust, coir pith and many organic wastes are successfully chemical activated at low temperatures and reportedly used for the removal of heavy metals, organic compounds and dyes [13,14]. Sulphuration and nitrogenation of the activated carbon surface favour the adsorption of organic compounds, sulphur complexes onto the carbon surface; it increases the surface polarity and leads to a specific interaction with polar pollutants [15,16].

The present study includes the preparation of activated carbon from the agricultural byproduct *Areca triandra* palm shell (ATPS), a novel and unconventional precursor, by low temperature sulphuric acid activation, evaluation of the physical and surface chemical properties, and the adsorption of methylene blue dye onto the prepared adsorbent.

2. Materials and methods

2.1. Adsorbent preparation

The ATPS obtained from a solid waste disposal of a nut cracking unit near Wayanad, a town in south India was used as the precursor. It is washed, cleaned and dried in a hot air oven at 105°C for 6–8 h before activation. The ATPS was crushed and sieved for 1–2-mm size particles. Concentrated H_2SO_4 was then added to the weight ratio 1:2 (ATPS: Conc. H_2SO_4) and mixed thoroughly in a beaker. The beaker was kept in hot air oven at 120°C for 12 h. After the activation, the contents were cooled to room temperature in a desiccator. The carbonated ATPS was washed with 5% $NaHCO_3$ solution to remove the traces of acid and with excess double-distilled water until the pH stabilizes. After washing, it is dried in a hot air oven at 105°C for 6 h and cooled to room temperature in a desiccator. The carbonized areca triandra shell adsorbent (CATPS) was crushed, size separated and stored in an airtight container for characterization and adsorption studies.

2.2. Effluent preparation

The methylene blue (MB) used is a basic (cationic) dye supplied by Merck, has the formula $C_{16}H_{18}ClN_3S$, molecular weight 319.86 g/mol, molecular volume 241.9 cm^3/mol and molecular diameter 0.8 nm with a heterocyclic aromatic molecular structure.

A stock MB solution of 1,000 mg/L was prepared by dissolving 1,000 mg of MB with double-distilled water in a 1,000-mL standard measuring flask. Standard solutions of required concentrations were prepared from the stock solution by diluting with double-distilled water.

2.3. Analytical characterizations

The elemental composition of ATPS was analysed using CHNS Analyzer (Vario EL III, Elementar, Germany), ICP-AES (Thermo Electron IRIS INTREPID II XSP DUO) and EDX. The BET surface area and pore structure of the CATPS were determined using a BET surface area analyser (NOVA, Quantachrome Instruments, USA). The surface morphology of the samples was examined by a Scanning Electron Microscope (SEM with EDX) (Hitachi SU-6600, Japan). The surface functional groups of ATPS, CATPS and CATPS–MB (after adsorption with MB) were analysed using FT-IR spectrophotometer (JASCO Analytical Instruments FT-IR 6300, USA), the IR spectra were recorded in the wave number range of 400–4,000 cm^{-1}.

2.4. Boehm titrations

The oxygen surface functional groups were estimated using a set of redox titrations referred to as Boehm titrations. The value of acidic sites was determined by the assumptions that the strong base NaOH neutralizes Bronsted acids (e.g. carboxylic, lactonic and phenolic groups), and Na_2CO_3 could neutralize carboxylic and lactonic groups, while $NaHCO_3$ neutralizes only carboxylic groups [17]. 300 mg of adsorbent sample was mixed with 25 mL of each of the following solutions, sodium hydroxide (0.1 mol/L), sodium carbonate (0.05 mol/L), sodium bicarbonate (0.1 mol/L) and hydrochloric acid (0.1 mol/L). The bottles were then stoppered and kept in an orbital shaker for 24 h. The solutions are then filtered and 10 mL of each base solution was titrated against HCl (0.1 mol/L), and the acid solution was titrated against 0.1 mol/L NaOH. The amount of various bases and acids neutralized by the adsorbent surface quantitatively represents the surface functional groups.

2.5. Point of zero charge (pH_{PZC})

The pH_{PZC} is an important electrochemical property of an adsorbent; its value depends on the net total surface charge of the adsorbent particles, it is defined as the pH at which the carbon surface has no charge in the absence of specific adsorption. The pH_{PZC} of the CATPS is analysed using pH drift method [18]. 1,000 mL of freshly prepared double-distilled water was used to prepare 0.1 mol/L NaCl solution in order to eliminate traces of dissolved gases, to each 100 mL of this solution 0.1 mol/L NaOH or 0.1 mol/L HCl is added in suitable quantity to prepare solutions with 2, 4, 6, 8, 10 and 12 pHs (pH_i). 150 mg of dried CATPS was added to 50 mL of each solution in a stoppered Erlenmeyer's flask and well mixed in an orbital shaker at 150 rpm for 48 h. Later, the final pH (pH_f) of each solution is measured and plotted against pH_i, the point of intersection of the diagonal pH_i line and the pH_f curve is noted as pH_{PZC}.

2.6. Batch adsorption studies

The batch adsorption studies were carried out in a series of 250-mL stoppered Erlenmeyer flasks containing 100 mL of MB solution. Experiments were conducted to study the effect of various process parameters, such as contact time (t), adsorbate concentration (5–20 mg/L), adsorbent dosage (0.5–2 g/L) and solution pH (2–12) at a constant agitation speed of 150 rpm in a thermostated incubator shaker. The pH of the dye solution was adjusted to the required value using 0.1 mol/L HCl or 0.1 mol/L NaOH solution. Samples were collected at the interval of 10 min until equilibrium and analysed for absorbance at 665 nm wavelength in a UV–vis spectrophotometer. All batch adsorption studies were carried out using CATPS with an average particle size of 0.137 mm (100–120 mesh). The percentage removal of MB (removal %) and the adsorption capacity (q_e—mg/g) for each concentration of MB at equilibrium were calculated from known, effluent volume (L), adsorbent mass (g), initial concentration C_0 (mg/L) and equilibrium concentration C_e (mg/L) of each run. Desorption studies were conducted to recover the MB from the adsorbent using different concentrations (0.0001, 0.001 and 0.01 mol/L) of HCl as eluting agent.

2.7. Isotherm models

The mechanism of adsorption is influenced by the nature of interaction between the adsorbate and adsorbing surface. This interaction is a result of chemical bonding, hydrogen bonding, hydrophobic and van der Waals forces [19]. The adsorption isotherms are used to explain and classify the interaction between a specific adsorbent–adsorbate pair. The CATPS and MB interactions are analysed based on the experiments conducted with 10 mg of CATPS added to each 250-mL Erlenmeyer flasks containing 100 mL of MB solutions at various concentrations (50–250 mg/L) and placed in an orbital shaker at 150 rpm at NTP for a period of 3 h and the resultant concentrations are analysed and substituted in the following models.

2.7.1. Langmuir isotherm model

The Langmuir Isotherm model assumes that the interaction between the adsorbate species and the adsorbing surface with homogeneous active sites is chemical in nature and forms a monolayer over the surface [20]. The Langmuir isotherm model is expressed by Eq. (1), where q_e and q_m (mg/g) are the amount of dye adsorbed per unit mass of sorbent at any instant and at equilibrium concentration (for complete monolayer formation), respectively, C_e (mg/L) is the equilibrium concentration of unadsorbed dye in solution at any instant and K_L (L/mg) is the Langmuir equilibrium constant related to the affinity of binding sites and energy of adsorption. A dimensionless separation factor R_L is given by Eq. (2), where C_0 (mg/L) is the highest initial concentration of the adsorbate. The value of the separation factor R_L indicates whether the isotherm type is unfavourable adsorption ($R_L > 1$), linear ($R_L = 1$), favourable ($0 < R_L < 1$) or irreversible ($R_L = 0$).

$$\frac{C_e}{q_e} = \frac{1}{K_L q_m} + \frac{C_e}{q_m} \tag{1}$$

$$R_L = \frac{1}{1 + K_L C_0} \tag{2}$$

2.7.2. Freundlich isotherm model

The Freundlich isotherm model equation describes adsorption with possible multilayer on a highly heterogeneous surface consisting of non-identical and energetically non-uniform sites [21]. The Freundlich model is expressed in Eq. (3). Where K_F (L/mmol) is the Freundlich isotherm constant, n is the intensity of adsorption and $n > 1$ favours the adsorption process.

$$q_e = K_F C_e^{1/n} \tag{3}$$

2.7.3. Temkin isotherm model

The Temkin isotherm model represents the binding heterogeneity. This model accounts the indirect adsorbate to adsorbate attractions in addition to the adsorbate–adsorbent interactions. This isotherm assumes that the heat of adsorption of all the molecules in the layer decreases linearly with coverage due to adsorbent–adsorbate interactions, and the adsorption is characterized by a uniform distribution of binding energies up to a limiting binding energy [22]. The Temkin isotherm model is expressed in Eq. (4). Where R (J/mol ˚K) the universal gas constant, T (˚K) the absolute temperature, B (J/mol) and A (L/g) are Temkin's constants related to heat of sorption and isotherm constant, respectively.

$$q_e = \frac{RT}{B} \ln(A C_e) \tag{4}$$

2.8. Kinetic models

The knowledge of adsorption kinetics is very essential for the choice and design of the sorption equipment. The appropriate kinetics equation is selected by testing the batch adsorption data with existing models. The batch adsorption data were obtained by adding 10 mg of CATPS to each 250-mL Erlenmeyer flasks with 100 mL of 20 mg/L for MB and placed in an orbital shaker at 150 rpm at NTP at different time intervals, the amount of dye adsorbed onto CATPS at each time interval was noted and used in the following kinetic models.

2.8.1. Pseudo-first-order kinetic model

The pseudo-first-order model is a first-order rate equation based on adsorption capacity [23], with the governing Eq. (5). Where q_e and q_t (mg/g) are the adsorption capacities at equilibrium and at any instant of time, respectively, k_{p1} (min^{-1}) is the pseudo-first-order rate constant for the kinetic model.

$$\frac{dq_t}{dt} = k_{p1}(q_e - q_t) \tag{5}$$

2.8.2. Pseudo-second-order kinetic model

This model proposes that the adsorption kinetic is second order, and the rate limiting step is the chemical reaction involving valent forces by mutual sharing or exchange of electrons, also that adsorption follows the Langmuir isotherm model [24,25]. The model is represented by Eq. (6), where, k_{p2} (g/(mg min)) is the pseudo-second-order rate constant.

$$\frac{dq_t}{dt} = k_{p2}(q_e - q_t)^2 \tag{6}$$

2.8.3. Intra-particle diffusion model

The intra-particle diffusion model or homogeneous solid diffusion model (HSDM) was proposed to describe mass transfer in an amorphous and homogeneous sphere. In many adsorption studies, solute uptake varies with $t^{1/2}$ rather than t. This model is used to test whether intra-particle diffusion is the sole limiting step of the adsorption process [19], and the governing equation is shown in Eq. (7) where k_{int} (min^{-1}) is the intra-particle diffusion rate constant.

$$q_t = k_{int} t^{1/2} \tag{7}$$

2.9. Continuous column studies

Packed bed column studies are essential to ensure the pertinence of the product in bulk adsorption in process plants [26,27]. The continuous studies were carried out in a glass column of 20 cm length and 1 cm diameter packed with 1 g of CATPS of an average particle size of 0.462 mm (35–40 mesh). The bed was nearly 1.2 cm in height and supported by glass wool at both the ends. MB dye solution of 100 mg/L was fed from the bottom of the column in order to maintain uniform wetting of the adsorbent, the flow rate was maintained at a steady flow of 5 mL/min with the help of a peristaltic pump. The outlet dye concentrations were noted at uniform time interval

Table 1
Surface functional groups of ATPS and CATPS

Material	Basic (mmol/g)	Carboxylic (mmol/g)	Lactonic (mmol/g)	Phenolic (mmol/g)
ATPS	0.2199	0.1153	0.1656	0.1863
CATPS	0.2666	0.4999	0.5667	0.1727

Table 2
CHNS analysis results of ATPS and CATPS

Material	C%	H%	N%	S%
ATPS	44.4	6.28	0.89	–
CATPS	43.0	2.47	0.56	0.63

and the operation of the column was carried out till the effluent reaches the inlet concentration.

2.10. Thermodynamic studies

The thermodynamic parameters were evaluated in order to confer the spontaneity, nature of reaction and randomness of the adsorption process. The effect of temperature on the Gibb's free energy change ($\Delta G°$) indicates the feasibility and spontaneity of the process [6]. The energy and entropy of the process also highlight the mechanism of adherence to the surface. The free energy $\Delta G°$ can be evaluated from b (L/mol) the Langmuir isotherm constant, R (8.314 J/mol K) universal gas constant and T (K) absolute temperature as follows:

$$\Delta G° = -RT \ln b \tag{8}$$

$\Delta H°$ (J/mol), the enthalpy change of adsorption and $\Delta S°$ (J/mol K), the entropy were estimated by the following equation:

$$\ln b = \Delta S°/R - \Delta H°/RT \tag{9}$$

The thermodynamic parameters for the adsorption of MB onto CATPS were evaluated by conducting batch adsorption studies at three different temperatures namely 301, 318 and 328 K in an isothermal shaker.

3. Results and discussion

3.1. Surface chemistry

The carbon surfaces are heterogenic in nature, acidic and basic functional groups coexist, so a series of Boehm titrations [17] were conducted to determine the type and concentration functional groups in raw ATPS and CATPS. The presence of carboxyl groups, lactones and hydroxyl groups of phenolic character contributes to the acidic nature of the surface and these groups differ in their acidities and the results are reported in Table 1. The strongly acidic carboxylic groups neutralized by $NaHCO_3$, lactone groups neutralized by Na_2CO_3 and the weak phenolic group react with strong alkali NaOH. The basic surface groups,

Table 3
FTIR analysis of CATPS before and after MB adsorption

Sl. no.	Peaks		Functional groups	Possible affinity for MB
	CATPS	CATPS–MB		
1	3,408	3,430	–OH bonded	[a]
2	2,922	2,924	CH_2	
3	2,851	2,854	CH_2	
4	1,710	1,715	C=O	[a]
5	1,642	1,630	C=O	[a]
6	1,584	1,598	Aromatic	[a]
7	1,384	1,384	SO_2	
8	1,111	1,117	SO_4^{2-}	[a]
9	1,022	1,019	Si–O–alkyl	[a]
10	776	–	CH_3	
11	607	609	SO_4^{2-}	[a]

[a]Indicating possible adsorbing group of MB.

pyrones and chromones are neutralized by HCl. Boehm titration results for CATPS showed that the concentration of acidic sites is several times higher than the basic groups. The treatment of H_2SO_4 increased the acid groups and provided more oxygenated functionality which in turn favours the affinity for cationic MB [28].

FTIR spectra of raw ATPS showed characteristics similar to common plant-based lignocellulosic biomass. The CHNS analysis of raw ATPS and CATPS also confirmed the features of carbonaceous biomass as shown in Table 2 and the ICP-AES analysis shows the presence of trace elements Ca—5.275 g/kg, Na—0.36 g/kg and Si—0.28 g/kg in the raw ATPS. FTIR spectroscopy was used to obtain the information regarding the chemical structure and functional groups of ATPS and CATPS. The infrared absorption bands of CATPS and CATPS–MB and the corresponding functional groups are shown in Table 3.

The FTIR spectrum of CATPS and CATPS–MB shows a broad band at $3,408$ cm^{-1} and indicates the presence of hydrogen bonded hydroxyls involved in phenolic groups. The doublet, approximately with a separation of 80 cm^{-1} at 2,922 and 2,851 cm^{-1} indicates aliphatic CH_2 groups. Near the wave number $1,710$ cm^{-1}, appears a shoulder and a trough at $1,642$ cm^{-1} noticed for CATPS which may be caused by the carbonyl stretch of carboxyl group [3]. The two bands separated by about 180 cm^{-1} between 1,384 and $1,200$ cm^{-1} indicate SO_2 group. The SO_4^{2-} groups absorb at $1,111$ cm^{-1}. The sulphate ion SO_4^{2-} has its bending band at 607 cm^{-1}. The IR analysis suggests that sulphuric acid chemical activation leads to the incorporation of sulphur element in the structure of the carbon. Table 3 shows the surface functional groups created by the treatment process and indicates
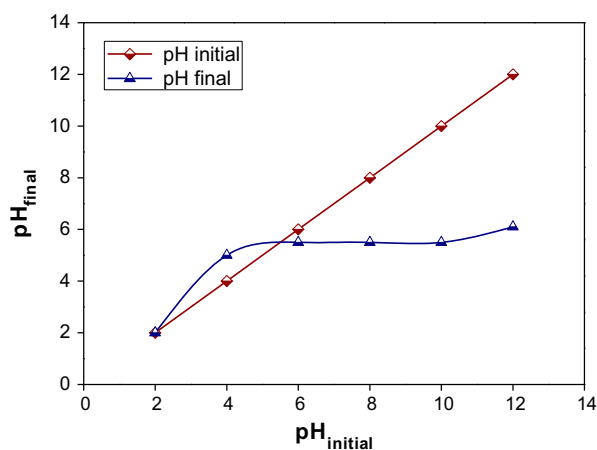
the possible functional groups involved in the adsorption process, which possess physical or chemical affinity for MB.

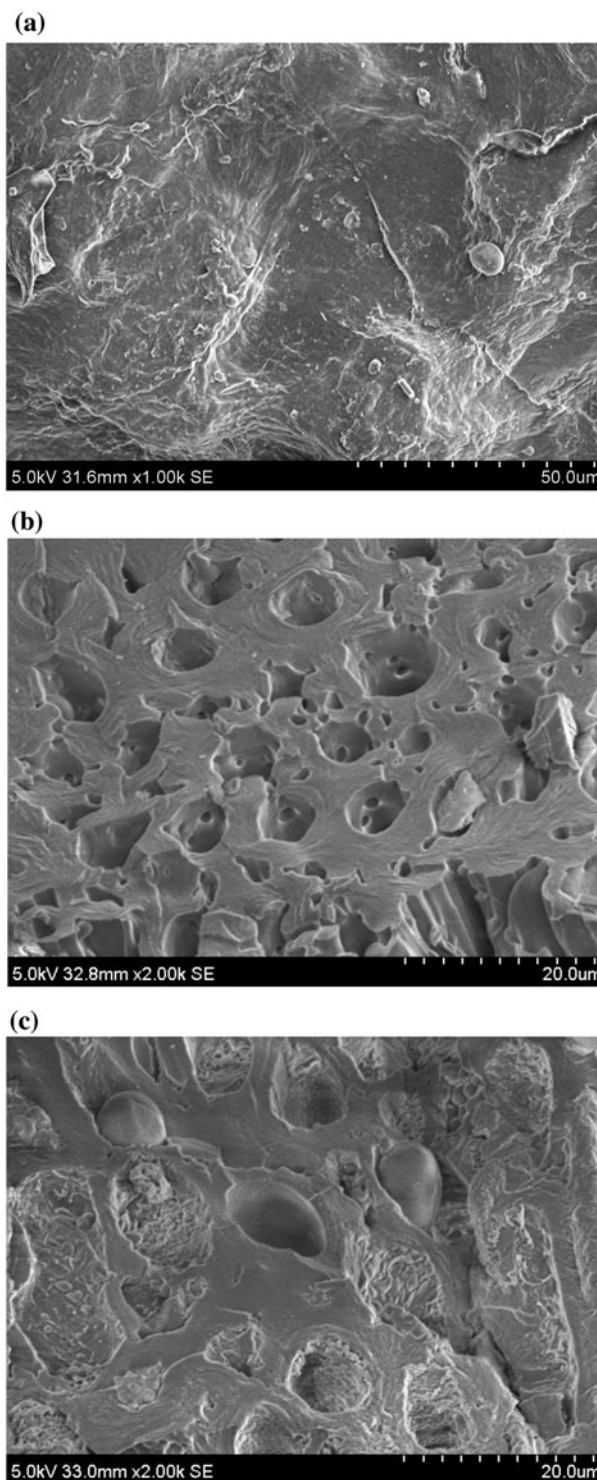Fig. 2. SEM image of (a) ATPS, (b) CATPS and (c) CATPS–MB.

Fig. 1. Point of zero charge of CATPS.

The point of zero charge (pH_{PZC}) accounts for the coulombs interaction between the carbon surface and the adsorbate in the liquid phase. The pH_{PZC} value for CATPS is found to be 5.5 pH (Fig. 1) which indicates that the surface is acidic in nature [14], implying the extent of oxidation on the surface [18]. The surface acquires a net negative charge above 5.5 pH and a higher solution pH enhances the MB adsorption.

3.2. BET analysis

The BET surface area is an important microstructural analysis used for determining the specific surface area and pore structure of materials. The specific surface area is directly related to the adsorption sites available, which in turn provides insight into the sorption potential of a substance. The BET surface area, average pore volume and pore diameter of the CATPS are determined with nitrogen gas at −196℃. The CATPS prepared has a BET surface area of 27.3 m²/g, pore volume of 0.0419 cc/g and an average pore diameter of 5.075 nm, which indicates that the adsorbent is mesoporous as defined by IUPAC (International Union of Pure & Applied Chemistry) [29], which is reportedly the characteristic result of sulphuration [16,30,31].

3.3. Surface morphology

Scanning electron microscopy was employed to visualize the surface morphology, pore structure and structural changes of ATPS, CATPS and CATPS–MB. The SEM image of the raw material ATPS Fig. 2(a) shows that the surface is dense and planar without any pores, with numerous fibrous veins running all over the surface. Energy-dispersive X-ray spectroscopy, (EDX) a peripheral device of SEM assembly, estimated the information about the chemical composition of ATPS (C—37.91%, O—54.16%, Si—0.53% and Ca—7.4%) by evaluating the energy of the X-rays released by the interaction between electron beam and the constituent atoms of ATPS. Fig. 2(b) shows that the CATPS has a regular well-defined homogeneous pore structure arrangement; with a well-developed
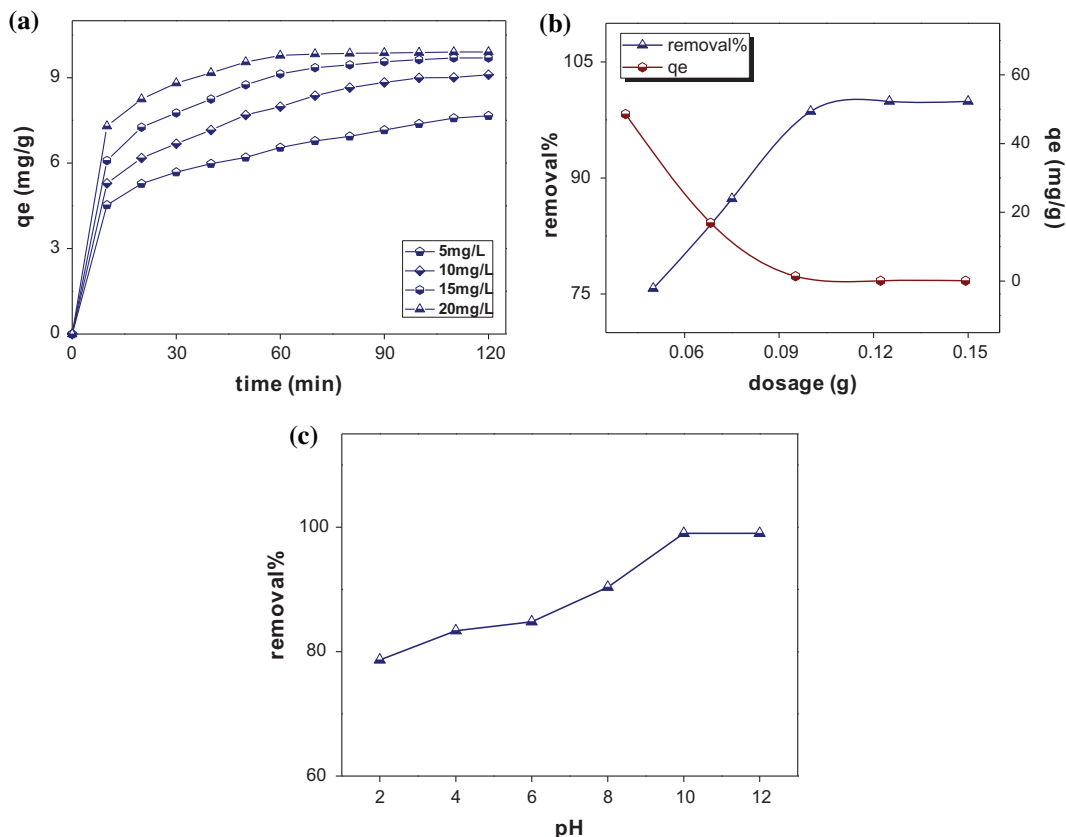

Fig. 3. Effect of (a) initial concentration with contact time, (b) CATPS dosage and (c) pH for the adsorption of MB onto CATPS.

Table 4
Isotherm model constants and coefficients for MB adsorption onto CATPS

Isotherm model	Parameters	R^2
Langmuir	$K_L = 0.0259$ L/mg; $R_L = 0.133$	0.99
Freundlich	$K_F = 31.22$ L/mmol; $n = 2.445$	0.95
Temkin	$A = 0.2107$ dm^3/g; $B = 68.951$	0.97

honeycomb-like morphology. The SEM image of CATPS before and after adsorption (Fig. 2(b) and (c)) of MB shows a marked difference [3].

3.4. Effect of contact time

Adsorption equilibrium is a condition at which there is no significant change in concentration of dye in the aqueous phase with a corresponding increase in contact time. The adsorption percentage of MB dye increased with the increase in contact time as in Fig. 3(a). The removal of MB was found to be rapid at the initial period and then becomes slow and stagnant with the increase in time. The initial rapid adsorption of MB by CATPS might be due to affinity for acidic surface functional groups of CATPS [3,32].

3.5. Effect of initial concentration

The adsorption capacity was found to increase with an increase in the initial concentration of MB as shown in Fig. 3(a). With the agitation speed held constant for all solutions, the increase in dye uptake is increased with an increase in driving force, the concentration gradient between aqueous phase and adsorbent surface [3,32].

3.6. Effect of CATPS dosage

The influence of CATPS dosage on the removal efficiency and the adsorption capacity of MB is shown in Fig. 3(b). The removal efficiency increases with an increase in the dosage as the adsorption sites are more with a higher dosage. However, the adsorption capacity decreases with an increase in the dosage as the MB per weight of CATPS reduces.

3.7. Effect of pH

The effect of pH of dye solutions on the MB removal efficiency of CATPS is shown in Fig. 3(c). The MB percentage removal increases from 78 to 100% for an increase in solution pH from 2 to 10. The pH of the
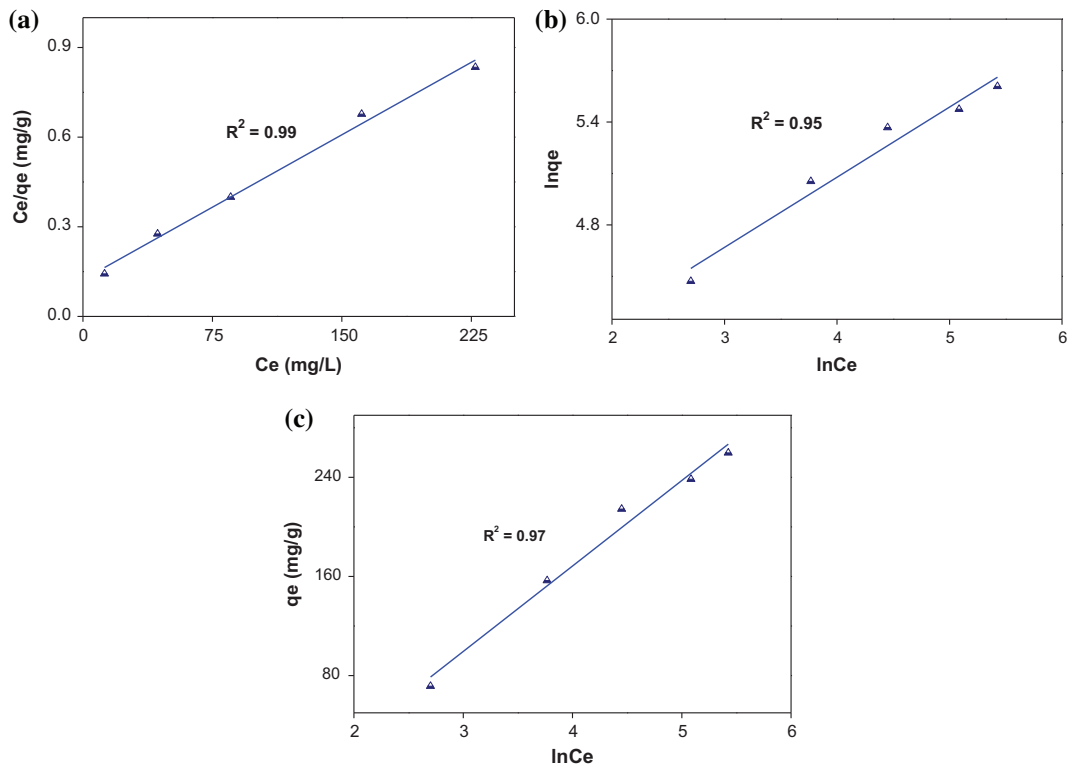

Fig. 4. Isotherm model fitness: (a) Langmuir, (b) Freundlich and (c) Temkin.

solution influences the surface charge of the adsorbent and dissociation of functional groups on its active site and degree of ionization of dye molecule. At high pH, the electrostatic attraction between the surface active sites of ATPS and the cationic MB molecule was increased due to the presence of hydroxyl and –COO$^-$ groups [33]. Regeneration studies conducted at different concentrations of HCl resulted in no desorption of MB back into solution, due to strong interaction.

3.8. Equilibrium isotherm models

In order to interpret the CATPS surface and MB dye molecule interactions, three isotherm models where tested for the equilibrium adsorption data, namely Langmuir, Freundlich and Temkin. The model parameters are summarized in Table 4. The linearized isotherm graphs are shown in Fig. 4(a)–(c). The Langmuir isotherm model is found to fit satisfactorily with a high correlation coefficient of 0.998. From the Langmuir isotherm plot, the CATPS maximum adsorption capacity at complete monolayer q_m was found to be 312.5 mg/g and the dimensionless separation factor R_L is 0.133, which indicates a favourable adsorption. Whereas, the Freundlich isotherm model

fits the experimental data with a linear regression correlation coefficient of only 0.95, the Freundlich model parameter n (=2.445) represents favourable adsorption intensity. Temkin's model fits the experimental data with a correlation coefficient of 0.97 which indicates that the adsorbate–adsorbate interaction is negligible. From the analysis of the three isotherm models it can be concluded that adsorption of MB on CATPS is monolayer with uniform activity distribution.

3.9. Adsorption kinetic models

The mechanism of liquid phase adsorption is expressed by the kinetic models. Three kinetic models namely pseudo-first order, pseudo-second-order and intra-particle diffusion were tested to interpret the overriding mechanism. The linearized model graphs of the three models are shown in Fig. 5(a)–(c). The pseudo-second-order kinetic model fits the experimental data of CATPS–MB adsorption with a high correlation coefficient of 0.998, the surface reaction is the rate controlling step of the overall process, which suggests that there is a significant effect of the valence forces caused by sharing or exchange of electrons between the surface and the dye molecule [24]. The fit of
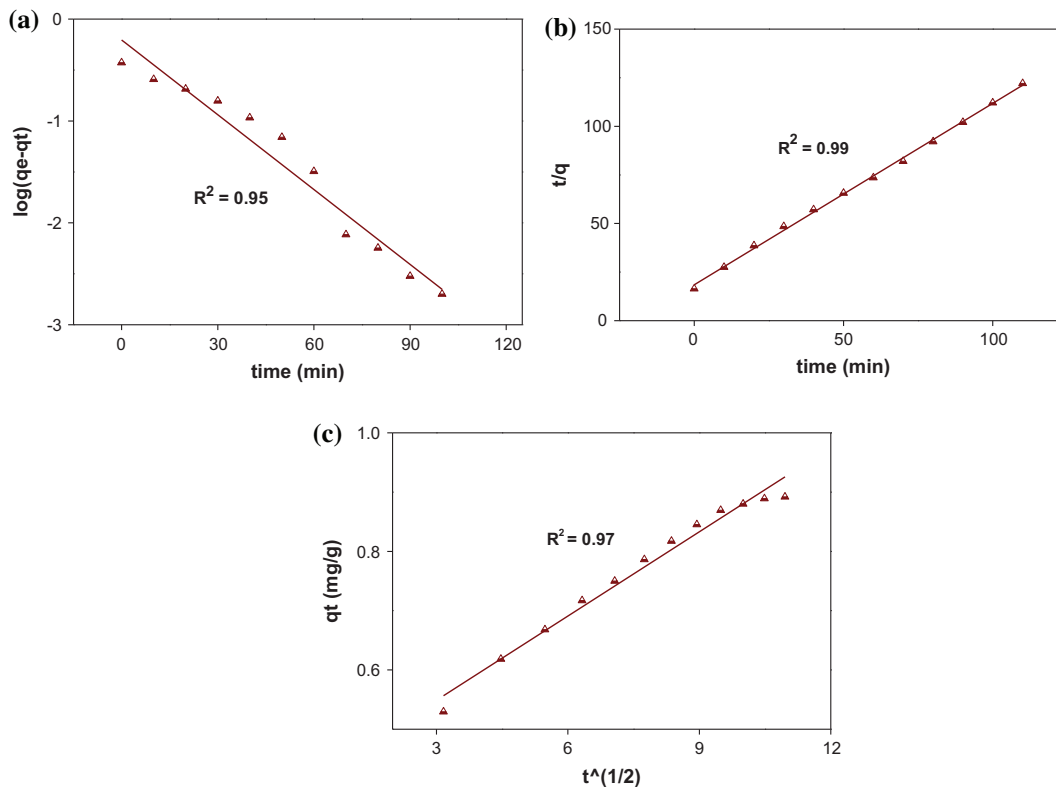

Fig. 5. Kinetic model fitness: (a) pseudo-first-order, (b) pseudo-second-order and (c) intra-particle diffusion models.

Table 5
Kinetic model constants and coefficients for MB adsorption on CATPS

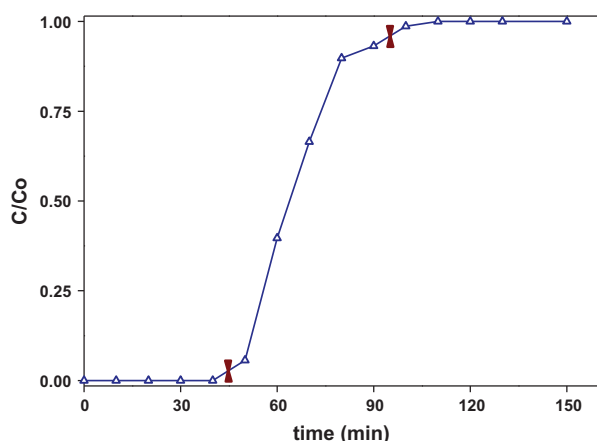| Kinetic model	Parameters	R^2
Pseudo-first-order	k_{p1} = 0.0563 min^{-1}; q_e = 0.6237 mg/g	0.95
Pseudo-second-order	k_{p2} = 0.0439 g/mg min; q_e = 1.0717 mg/g	0.99
Intra-particle diffusion	k_{int} = 0.0474 g/mg min$^{1/2}$	0.97

Fig. 6. Breakthrough curve for continuous column adsorption.

Table 6
Thermodynamic parameters for MB adsorption onto CATPS

T (K)	$\Delta G°$ (kJ/mol)	$\Delta H°$ (kJ/mol)	$\Delta S°$ (J/mol K)
301	−18.790		
318	−25.421	88.145	355.58
328	−28.242		

first-order Lagergren model with the experimental data resulted in a low correlation coefficient of 0.95, which suggests that the film diffusion is not the controlling step of this process [24]. The results showed that the intra-particle diffusion is not controlling the adsorption of MB on CATPS. From the kinetic model analysis it can be concluded that the kinetics of MB adsorption is second order with chemical interactions between dye and CATPS surface and the kinetic model parameters are listed in Table 5.

3.10. Column study

The packed column adsorption study was conducted to test the applicability of CATPS as adsorbent in the continuous adsorption process using a simulated MB solution. The breakthrough curve is shown in Fig. 6. From the breakthrough curve it was observed that a packed bed column with 1 g of CATPS was able to treat 232 mL of MB solution of 100 mg/L concentration. The result suggests that CATPS can be used as a potential adsorbent for the removal of industrial effluent.

3.11. Thermodynamic parameters

The thermodynamic parameters obtained for MB on CATPS are presented in Table 6. The negative Gibb's free energy ($\Delta G°$) values for all the temperature suggest that the adsorption is feasible and spontaneous, also the values of $\Delta G°$ were found to decrease with an increase in temperature construe that higher temperature favours MB adsorption onto CATPS. The enthalpy change ($\Delta H°$) has a positive value (88.145 kJ/mol) representing that the adsorption is an endothermic process which supported the observation that increase in adsorption rate with an increase in temperature. Also the positive value (355.58 J/mol K) of entropy ($\Delta S°$) confirmed the increased randomness at the CATPS–MB interface, indicating the MB ions have replaced the previously adsorbed water molecules at the CATPS surface with a more prominent affinity [34,35].

4. Conclusions

In the present study, an adsorbent was prepared from ATPS by chemical activation using sulphuric acid and was successfully subjected for the adsorption of MB. The studies demonstrate that by low temperature activation of ATPS with sulphuric acid produced a characteristic mesoporous adsorbent. The adsorbent surface functional groups were identified as hydroxyl, carboxyl, lactonic SO_4^- and some basic functional groups. The adsorption of MB ions is favoured at a higher pH. The equilibrium adsorption data were well fitted by the Langmuir isotherm model, indicative of monolayer adsorption by CATPS. Kinetic adsorption studies revealed that the adsorption process is described by pseudo-second-order kinetics, which suggest that the process is controlled by chemical

reaction. The negative values of Gibb's free energy change ($\Delta G°$) reinforce the spontaneous process, the positive enthalpy change ($\Delta H°$) confirms that the process is endothermic and positive entropy ($\Delta S°$) vindicates the strong affinity for MB. The bulk adsorption study suggests that the adsorbent is suitable for the continuous packed bed adsorption. Therefore, it can be concluded that CATPS can be employed as an effective adsorbent for the removal of cationic MB from aqueous solution.

List of symbols

A	—	Temkin isotherm constant (L/g)
b	—	Langmuir isotherm constant (L/mol)
B	—	Temkin isotherm constant related to heat of adsorption (J/mol)
C_e	—	concentration of the solute in the solution at equilibrium (mg/L)
C_0	—	concentration of the solute in the solution initially (mg/L)
$\Delta G°$	—	Gibb's free energy change (kJ/mol)
$\Delta H°$	—	enthalpy change (kJ/mol)
k_{int}	—	intra-particle diffusion rate constant (min^{-1})
k_{p1}	—	pseudo-first-order rate constant (min^{-1})
k_{p2}	—	pseudo-second-order rate constant (g/(mg min))
K_F	—	Freundlich isotherm equilibrium constant (L/mmol)
K_L	—	Langmuir isotherm equilibrium constant (L/mg)
M	—	weight of the adsorbent (g)
n	—	intensity of adsorption dimensionless
q_e	—	equilibrium adsorption capacity (mg/g)
q_m	—	maximum adsorption capacity at complete monolayer (mg/g)
q_t	—	adsorption capacity at any time (mg/g)
R	—	universal gas constant (8.314×10^{-3} kJ/kmol)
R_L	—	Langmuir dimensionless separation factor
$\Delta S°$	—	entropy change (J/mol K)
t	—	time (min)
T	—	absolute temperature (K)
V	—	volume of the solution (L)

References

[1] T. Robinson, G. McMullan, R. Marchant, P. Nigam, Remediation of dyes in textile effluent: A critical review on current treatment technologies with a proposed alternative, Bioresour. Technol. 77 (2001) 247–255.

[2] Ö. Tunç, H. Tanacı, Z. Aksu, Potential use of cotton plant wastes for the removal of Remazol Black B reactive dye, J. Hazard. Mater. 163 (2009) 187–198.

[3] A. Ahmad, M. Rafatullah, O. Sulaiman, M.H. Ibrahim, R. Hashim, Scavenging behaviour of meranti sawdust in the removal of methylene blue from aqueous solution, J. Hazard. Mater. 170 (2009) 357–365.

[4] D. Mitrogiannis, G. Markou, A. Çelekli, H. Bozkurt, Biosorption of methylene blue onto *Arthrospira platensis* biomass: Kinetic, equilibrium and thermodynamic studies, J. Environ. Chem. Eng. 3 (2015) 670–680.

[5] M. Ghaedi, S.N. Kokhdan, Removal of methylene blue from aqueous solution by wood millet carbon optimization using response surface methodology, Spectrochim. Acta, Part A 136 (2015) 141–148.

[6.] A. Mittal, Adsorption kinetics of removal of a toxic dye, Malachite Green, from wastewater by using hen feathers, J. Hazard. Mater. 133 (2006) 196–202.

[7] P. Sudamalla, S. Pichiah, M. Manickam, Responses of surface modeling and optimization of Brilliant Green adsorption by adsorbent prepared from *Citrus limetta* peel, Desalin. Water Treat. 50 (2012) 367–375.

[8] A. Mittal, Use of hen feathers as potential adsorbent for the removal of a hazardous dye, Brilliant Blue FCF, from wastewater, J. Hazard. Mater. 128 (2006) 233–239.

[9] M.A.M. Salleh, D.K. Mahmoud, W.A. Wan Abdul Karim, A. Idris, Cationic and anionic dye adsorption by agricultural solid wastes: A comprehensive review, Desalination 280 (2011) 1–13.

[10] J. Mittal, D. Jhare, H. Vardhan, A. Mittal, Utilization of bottom ash as a low-cost sorbent for the removal and recovery of a toxic halogen containing dye eosin yellow, Desalin. Water Treat. 52 (2014) 4508–4519.

[11] A. Ismail, D.B. Adie, I.A. Oke, J.A. Otun, N.O. Olarinoye, S. Lukman, C.A. Okuofu, Adsorption kinetics of cadmium ions onto powdered corn cobs, Can. J. Chem. Eng. 87 (2009) 896–909.

[12] H. Daraei, A. Mittal, M. Noorisepehr, J. Mittal, Separation of chromium from water samples using eggshell powder as a low-cost sorbent: Kinetic and thermodynamic studies, Desalin. Water Treat. 53 (2015) 214–220.

[13] Y. Liu, J. Wang, Y. Zheng, A. Wang, Adsorption of methylene blue by kapok fiber treated by sodium chlorite optimized with response surface methodology, Chem. Eng. J. 184 (2012) 248–255.

[14] K.A.G. Gusmão, L.V.A. Gurgel, T.M.S. Melo, L.F. Gil, Adsorption studies of methylene blue and gentian violet on sugarcane bagasse modified with EDTA dianhydride (EDTAD) in aqueous solutions: Kinetic and equilibrium aspects, J. Environ. Manage. 118 (2013) 135–143.

[15] W. Feng, E. Borguet, R.D. Vidic, Sulfurization of carbon surface for vapor phase mercury removal—I: Effect of temperature and sulfurization protocol, Carbon 44 (2006) 2990–2997.

[16] J. Rivera-Utrilla, M. Sánchez-Polo, V. Gómez-Serrano, P.M. Álvarez, M.C.M. Alvim-Ferraz, J.M. Dias, Activated carbon modifications to enhance its water treatment applications. An overview, J. Hazard. Mater. 187 (2011) 1–23.

[17] N. Zhao, N. Wei, J. Li, Z. Qiao, J. Cui, F. He, Surface properties of chemically modified activated carbons for adsorption rate of Cr(VI), Chem. Eng. J. 115 (2005) 133–138.

[18] C.O. Ania, J.B. Parra, J.J. Pis, Influence of oxygen-containing functional groups on active carbon adsorption of selected organic compounds, Fuel Process. Technol. 79 (2002) 265–271.

[19] Y. Rajesh, M. Pujari, R. Uppaluri, Equilibrium and kinetic studies of Ni(II) adsorption using pineapple and bamboo stem based adsorbents, Sep. Sci. Technol. 49 (2014) 533–544.

[20] B.H. Hameed, Evaluation of papaya seeds as a novel non-conventional low-cost adsorbent for removal of methylene blue, J. Hazard. Mater. 162 (2009) 939–944.

[21] A. Mittal, R. Ahmad, I. Hasan, Iron oxide-impregnated dextrin nano-composite: Synthesis and its application for the biosorption of Cr(VI) ions from aqueous solution, Desalin. Water Treat. (2015) 1–13. doi: 10.1080/19443994.2015.1070764.

[22] H. Zheng, D. Liu, Y. Zheng, S. Liang, Z. Liu, Sorption isotherm and kinetic modeling of aniline on Cr–bentonite, J. Hazard. Mater. 167 (2009) 141–147.

[23] Y.S. Ho, G. McKay, A comparison of chemisorption kinetic models applied to pollutant removal on various sorbents, Process Saf. Environ. Prot. 76(4) (1998) 332-340

[24] Y.S. Ho, G. McKay, Pseudo-second order model for sorption processes, Process Biochem. 34 (1999) 451–465.

[25] Y.S. Ho, G. Mckay, Kinetic models for the sorption of dye from aqueous solution by wood, Process Saf. Environ. Prot. 76(2) (1998) 183–191.

[26] G.L. Dotto, J.M. Santos, R. Rosa, L.A.A. Pinto, F.A. Pavan, E.C. Lima, Fixed bed adsorption of Methylene Blue by ultrasonic surface modified chitin supported on sand, Chem. Eng. Res. Des. 100 (2015) 302–310.

[27] Mu. Naushad, A. Mittal, M. Rathore, V. Gupta, Ion-exchange kinetic studies for Cd(II), Co(II), Cu(II), and Pb(II) metal ions over a composite cation exchanger, Desalin. Water Treat. 54 (2015) 2883–2890

[28] Z. Wang, M.D. Shirley, S.T. Meikle, R.L.D. Whitby, S.V. Mikhalovsky, The surface acidity of acid oxidised multi-walled carbon nanotubes and the influence of in-situ generated fulvic acids on their stability in aqueous dispersions, Carbon 47 (2009) 73–79.

[29] B.K. Pradhan, N.K. Sandle, Effect of different oxidizing agent treatments on the surface properties of activated carbons, Carbon 37 (1999) 1323–1332.

[30] K. Anoop Krishnan, T.S. Anirudhan, Removal of mercury(II) from aqueous solutions and chlor-alkali industry effluent by steam activated and sulphurised activated carbons prepared from bagasse pith: Kinetics and equilibrium studies, J. Hazard. Mater. 92 (2002) 161–183.

[31] H.-C. His, C.-T. Chen, Influences of acidic/oxidizing gases on elemental mercury adsorption equilibrium and kinetics of sulfur-impregnated activated carbon, Fuel 98 (2012) 229–235.

[32] S. Karagoz, T. Tay, S. Ucar, M. Erdem, Activated carbons from waste biomass by sulfuric acid activation and their use on methylene blue adsorption, Bioresour. Technol. 99 (2008) 6214–6222.

[33] M. Auta, B.H. Hameed, Chitosan–clay composite as highly effective and low-cost adsorbent for batch and fixed-bed adsorption of methylene blue, Chem. Eng. J. 237 (2014) 352–361.

[34] S. Hong, C. Wen, J. He, F. Gan, Y.-S. Ho, Adsorption thermodynamics of Methylene Blue onto bentonite, J. Hazard. Mater. 167 (2009) 630–633.

[35] Y. Bulut, H. Aydın, A kinetics and thermodynamics study of methylene blue adsorption on wheat shells, Desalination 194 (2006) 259–267.